Sustainable Energy Technologies and Assessments 25 (2018) 146–160

Contents lists available at ScienceDirect

Sustainable Energy Technologies and Assessments

journal homepage: www.elsevier.com/locate/seta

Prediction of wind speed and wind direction using artificial neural network, support vector regression and adaptive neuro-fuzzy inference system

A. Khosravi*, R.N.N. Koury, L. Machado, J.J.G. Pabon

Postgraduate Program in Mechanical Engineering, Federal University of Minas Gerais (UFMG), Belo Horizonte, Brazil

ARTICLE INFO

Keywords:
Wind energy
Wind direction
Support vector regression
ANFIS
Partial swarm optimization

ABSTRACT

In this study, three models of machine learning algorithms are implemented to predict wind speed, wind direction and output power of a wind turbine. The first model is multilayer feed-forward neural network (MLFFNN) that is trained with different data training algorithms. The second model is support vector regression with a radial basis function (SVR-RBF). The third model is adaptive neuro-fuzzy inference system (ANFIS) that is optimized with a partial swarm optimization algorithm (ANFIS-PSO). Temperature, pressure, relative humidity and local time are considered as input variables of the models. A large set of wind speed and wind direction data measured at 5-min, 10-min, 30-min and 1-h intervals are utilized to accurately predict wind speed and its direction for Bushehr. Energy and exergy analysis of wind energy for a wind turbine (E-44, 900 kW) is done. Also, the developed models are used to predict the output power of the wind turbine. Comparison of the statistical indices for the predicted and actual data indicate that the SVR-RBF model outperforms the MLFFNN and ANFIS-PSO models. Also, the current energy and exergy analysis presents an average of 32% energy efficiency and approximately 25% exergy efficiency of the wind turbine in the study region.

Introduction

The increasing concern about air pollution, global warming and energy crisis will inevitably result in a transition in energy section from fossil fuel-based mode to renewable and non-polluting mode. Between the renewable energies, the wind energy is more accessible and fairly cheaper [1]. Wind energy is a clean resource and doesn't pollute the air like fossil fuel power stations. In addition, it doesn't produce atmospheric emissions which increase health problems. Power produced by wind turbines (WTs) depends on wind speed and its direction. Due to the importance of short-term prediction of the wind speed for connecting and disconnecting the power to the grid and management of the power, some scholars implemented machine learning algorithms to this target [2–4]. Artificial neural network (ANN) is a kind of machine learning algorithm that is proposed to predict wind speed and its direction [4–11].

Many studies proposed meteorological data, e.g., pressure, temperature, relative humidity and etc., of each region, to predict the wind speed and its direction with ANN [12], [13]. Ref. [13] implemented ANN in order to predict short-term wind speed in Mardin, Turkey. A multilayer perceptron (MLP) neural network was used to predict the wind speed by them. Mean square error (MSE) and correlation coefficient (R) were used as statistical parameters to evaluate the network that these indices were reported respectively by 0.3780 (m/s) and 0.9704. Ref. [14] applied fuzzy modeling technique and ANN to estimate annual energy output of a wind farm. Average wind speed, standard deviation of wind speed and air density of the study region were used as input variables of the models.

Ref. [15] developed an ANFIS model in order to estimate wind turbine power coefficient as a function of pitch angle and tip-speed ratio. It is shown, the proposed ANFIS model can successfully predict the wind turbine power coefficient. In a wind farm near central Taiwan area, radial basis function neural network based on a model with a feedback scheme error, for prognostication of wind speed and produced power, was developed by Ref. [16]. ANN based on multiple local measurements was used to predict wind speed in Eskisehir (Turkey) by Ref. [17]. Forecasting model was developed based on past values of wind speed data, temperature and pressure of the region as input variables. The best performance of the model was obtained in term of RMSE by 0.6940 (m/s).

Ref. [18] developed a generalized regression neural network (GRNN) in order to predict wind speed for the western region of India. The input variables of the model were longitude, latitude, daily horizontal solar irradiance, air temperature, relative humidity, earth temperature, elevation, cooling degree-days, heating degree-days and atmospheric pressure. Also, the GRNN was compared to an MLPNN and

* Corresponding author.
E-mail address: Alikhosraviis86@ufmg.br (A. Khosravi).

https://doi.org/10.1016/j.seta.2018.01.001
Received 24 September 2017; Received in revised form 1 December 2017; Accepted 1 January 2018

A	area (m^2)
ANN	artificial neural network
Cp	power efficiency
cp_a	air specific heat (kJ/kg K)
cp_v	vapor specific heat (kJ/kg K)
$\dot{E}x$	exergy flow rate (kW)
$MAPE$	mean absolute percentage error
MSE	mean square error
m	mass
$\dot{m}$	mass flow rate (kg/s)
P	power (kW)
$purelin$	linear transfer function
p	pressure (hPa)
ke	kinetic energy
R	regression coefficient
RH	relative humidity (%)
$RMSE$	root mean square error
S	entropy
t	time(s)
$tansig$	hyperbolic-tangent sigmoid
T	temperature (K)
v	wind speed (m/s)
WD	wind direction
z	height (m)

Greek Symbols

ρ	density (kg/m^3)
η	energy efficiency
η_{gb}	gearbox efficiency
η_g	generator efficiency
η_p	power electronics efficiency
ω	humidity ratio
α	constant coefficient
Ψ	exergy efficiency

Subscripts/Superscripts

$dest$	destruction
p	potential
ch	chemical
chi	chill
a	air
amb	ambient

the result illustrated that the GRNN is more accurate than the MLPNN.

Outlier correction algorithm, wavelet and extreme learning machine were implemented to estimate wind speed data by Ref. [19]. Forecasting wind speed data by a novel method based on Weibull distribution was done by Ref. [20]. They developed a model based on Weibull and Gaussian probability distribution functions to estimate short-term wind speed data. The model was trained with recorded wind speed data of 2014 in Ankara (Turkey) and the developed model provided better forecasting compared to Weibull model. Also, some studies concentrated on the time-series wind speed prediction [21–23]. This forecasting model uses the past value of measured wind speed data in order to predict the wind speed in the future.

Support vector machines (SVMs) are classification and regression techniques, which optimize its structure based on the input data. These techniques for the first time have been introduced by Vapnik [24]. In recent years, SVM was successfully employed on classification tasks in

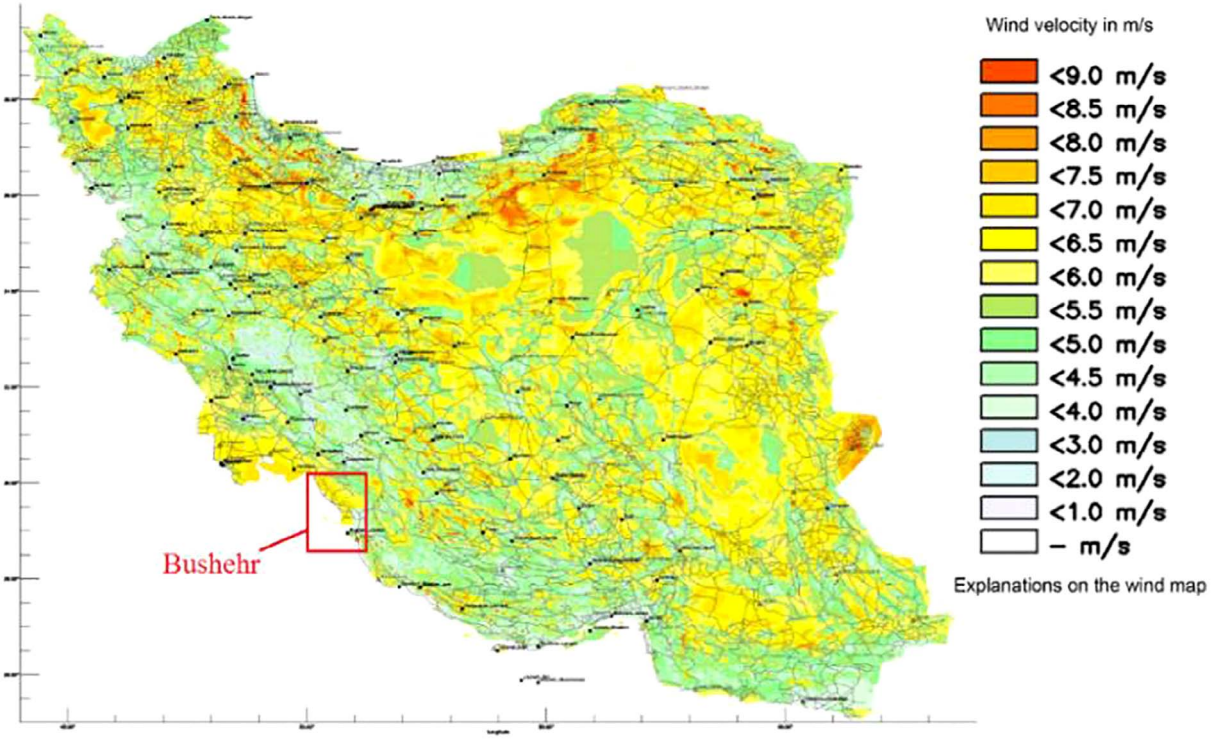

Fig. 1. Wind map of Iran.

very different areas of application. Support vector regression (SVR) is a subfield of SVM that uses the same principles of SVM with some minor differences. Several studies were implemented SVR to predict the wind speed or solar radiation [25–28]. Ref. [29] used an SVR model for prediction of mean 10-min time series data of wind speed. This model was compared to an MLPNN and the results demonstrated that both algorithms were applicable for estimation of wind speed time series data. Also, it was reported that the SVR model outperformed the MLPNN.

On the other hand, the current study represents an energy and exergy analysis of wind energy in the case study zone. Energy and exergy analysis is used to estimate the wind power potential in various worldwide regions [30–32]. Investigation of the wind energy potential in Turkey was implemented by Ref. [33], wherein the wind data from 23 different stations were collected and analyzed. Also, a similar study regarding exergy analysis of the wind turbine in Izmir (Turkey) was done by Refs. [34] and [35]. Ref. [36] evaluated exergy analysis of a wind farm in Southern Greece. The exergy analysis was implemented to identify the output actual energy from the existing available energy and also a wind map was designed by them. Ref. [37] investigated the effect of the meteorological data on the exergetic efficiency of WTs. Thermodynamic assessment of a WT based combined cycle carried out by Ref. [38]. They demonstrated that how a WT can be used to provide the energy of a compressor. Although most of the researchers implemented the first and second law of thermodynamics for several WTs in lots of stations, according to the fluctuation of the wind speed and variation of power producing patterns in each area, research is being continued in this issue [39–42].

The fossil fuel energy resource is gradually being replaced by renewable energy in the world. The sources of fossil fuel energy are limited and use of this resources causes the environmental pollutions and depletion of ozone layer [43]. Iran has primarily relied on a fossil fuel-based energy sector to make its country powerful. By looking at the meteorological data in Iran, it can be understood that there is a powerful potential for using the wind energy in this country. By considering these subjects, authors have been encouraged to evaluate the wind energy in this paper.

In this study, we investigate the idea of machine learning algorithms in order to predict wind speed, wind direction and output power of the WT (E44, 900 kW) in Bushehr that is located in the south of Iran. A novel method based on adaptive neuro-fuzzy inference system interconnected to a partial swarm optimization algorithm is developed to predict the targets. This type of the ANFIS model uses fuzzy c-means clustering to generate a fuzzy inference system. Considering the lake of enough investigations on the application of SVR model in wind speed and its direction, for this purpose, this research provides an accurate SVR technique to predict the targets. An MLFFNN with different data training algorithms is developed to obtain the better one. Also, the current study provides a comparison between the developed models. Finally, energy and exergy analysis of the wind energy for the WT is done.

Data analysis

In recent years, power generation of the wind energy in Iran had an impressive growth. In 2010, an amount of 203 MW of the Iran electricity demand was provided by wind power [44]. The average of wind speed for each area of Iran was provided as a wind map by renewable energy organization of Iran (Fig. 1) [45]. Analysis of the wind energy potential in 26 stations, with 33% energy efficiency, shows that an electrical energy of 6500 MW can be produced [45]. The case study is Bushehr that is located in the south of Iran (the red rectangle on the map, Fig. 1).

Fig. 2 indicates the meteorological data for Bushehr in 2016. Variation of the temperature (K) (a), relative humidity (%) (b), pressure (hPa) (c), and wind direction (WD) (deg) (d) for all day of the year are shown in this figure. Relative humidity and wind direction fluctuate each month or even each day. The trend of temperature between January to June is obviously increasing and after that is decreasing, whereas this trend for pressure is vice versa.

Fig. 3 demonstrates the variation of the wind speed (m/s) for Bushehr (Iran) between 2008 and 2016. Wind speed has different

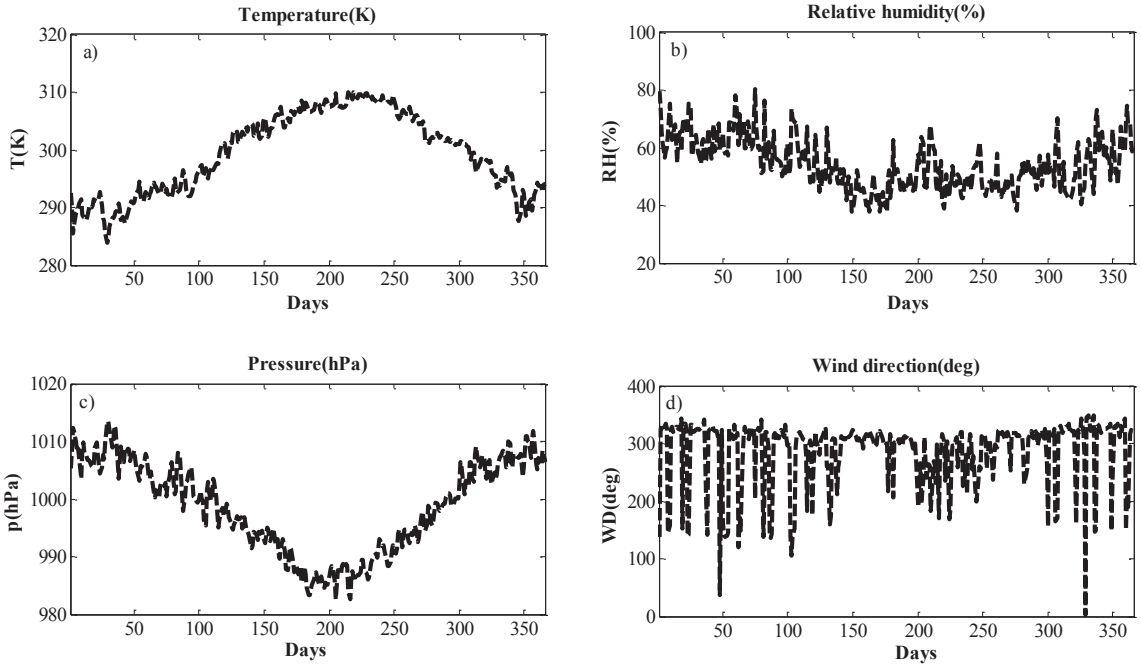

Fig. 2. Temperature (a), relative humidity (b), pressure (c), and wind direction (WD) (d) for Bushehr (Iran) in 2016.

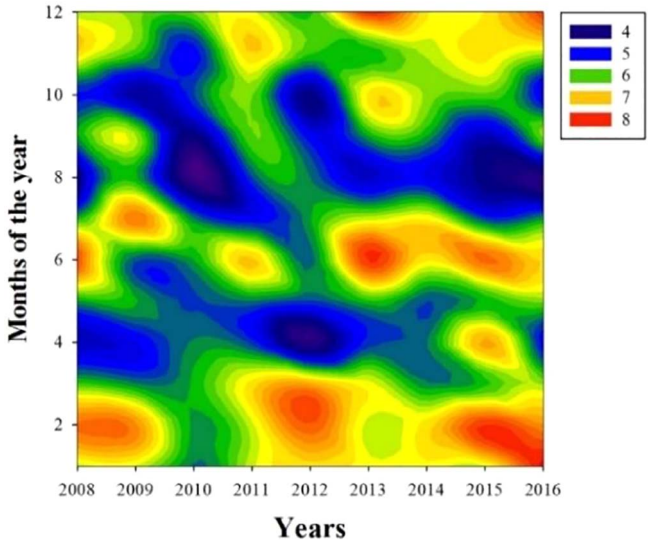

Fig. 3. Wind speed (m/s) for Bushehr (Iran) from 2008 to 2016.

varying patterns in different length of time, different height and different area. The timescale has an important significance for the study of wind power, and wind power studies under different time scales have different effects on the power system decision-making. The proposed models use the data that have been provided by NASA [46].

Forecasting models

Due to fluctuated nature of wind, prediction of the exact wind speed is necessary for relieving the disadvantageous impact to the grids. The mathematical model of the human brain that is inspired by the whole behavior of brain was obtained. Actually, this new scientific model is called ANN that is for mapping the relationship between the inputs and outputs. ANN not only has the good non-linear ability and the adaptive ability, and it also has the associative learning ability and strong fault tolerance. Therefore, in the aspect of forecasting, there is a large development space and good practical application for neural network. In this study, three methods of machine learning algorithms are implemented to predict the targets. Inputs of the models are local time (minute), temperature (K), pressure (hPa), and relative humidity (%) and the targets are wind speed (m/s), wind direction (deg) and output power of the WT (kW) (Fig. 4).

MLFFNN model

An MLFFNN is applied to predict wind speed and its direction. This model contains three layers: the first layer consists of a vector with four inputs; the second layer is hidden layer that contains a nonlinear transfer function (*tansig* is considered for this layer); the third layer is output layer contains a linear function (*purelin* is selected for this layer). For the current model, backpropagation algorithm is considered as training technique. This technique uses gradient-descent method for reducing the amount of the error(s) with adjusting the weight(s) and bias(s). An activation function for the MLFFNN with 4 inputs and one output is shown in Fig. 5. In this study, in order to obtain the maximum performance, different data training algorithms are considered. These algorithms are: Levenberg Marquardt (LM) (trainlm), BFGS Quasi-Newton (BFG) (trainbfg), Resilient Backpropagation (RP) (trainrp), Scaled Conjugate Gradient (SCG) (trainscg), Conjugate Gradient with Powell/Beale Restarts (CGB) (traincgb), Fletcher-Power Conjugate Gradient (CGF) (traincgf), Polak-Ribiere Conjugate Gradient (CGB) (traincgp), One-Step Secant (OSS) (trainoss) and Bayesian Regularization (BR) (trainbr).

SVR-RBF model

Support Vector Machines that have bee y_i n introduced by Vapnik (2013) [24] are classification and regression techniques, which optimize its structure based on the input data. For training data (x_i,y_i), …, (x_n,y_n), where x_i are the vectors with input values and y_i the appropriate output values for x_i, the ε-insensitive SVR aims to find a function $f(x)$, that has the deviation from the target at most ε at all times, while being as "flat" as possible. This problem can be written down as an optimization problem:

$$\min_{\omega,b,\xi,\xi^*} \frac{1}{2}\omega^T\omega + C\sum_{i=1}^{n}(\xi_i + \xi_i^*) \tag{1}$$

$$s.\ t.\begin{cases} y_i - (\langle\omega,x_i\rangle + b) \leqslant \varepsilon + \xi_i \\ (\langle\omega,x_i\rangle + b) - y_i \leqslant \varepsilon + \xi_i^* \\ \xi,\xi^* \geqslant 0 \end{cases} \tag{2}$$

In which, n is the number of samples, ξ_i shows the upper training error, ξ_i^* is the lower training error subject to the ε -insensitive tube $|y_i - (\langle\omega,x_i\rangle + b)|$. Also, C is the regularized constant that determines the trade-off between the regularization term and the empirical error, and $C > 0$. The SVR creates the $f(x)$ such that: (1) ξ_i and ξ_i^* are minimized to achieve the minimal training error and (2) to make the function "flat" and penalize too complex functions we minimize $\frac{1}{2}\omega^T\omega$. The final decision function is defined by:

$$f(x,\alpha_i,\alpha_i^*) = \sum_{i=1}^{n}(\alpha_i - \alpha_i^*)\kappa(x,x_i) + b \tag{3}$$

And can be found by utilizing the properties Lagrange multipliers, Kernel trick and the optimality constraints. The Lagrange multipliers and Kernel trick are described in Appendix B. For this study RBF is used as kernel function that its mapping space has an infinite number of dimensions.

ANFIS-PSO model

In order to obtain the knowledge of human expert for obtaining the fuzzy rules, an ANN is incorporated into a fuzzy system. This process is done by applying the learning algorithms for automatic fuzzy if-then rules generation and this connection (ANN into fuzzy system) is called neuro-fuzzy system [47]. Radial basis function type neural network (in

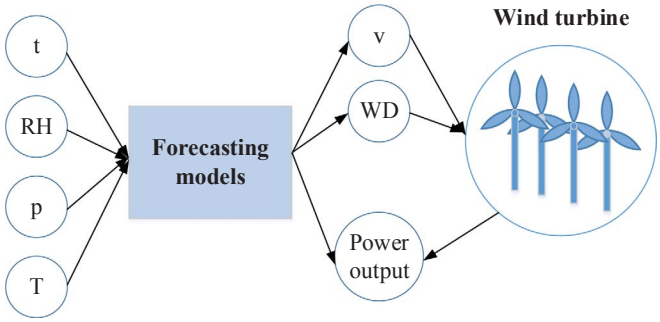

Fig. 4. Inputs and outputs variables of the forecasting models.

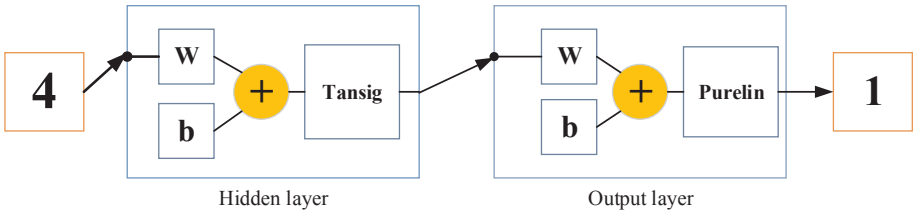

Fig. 5. Activation function for MLFFNN model.

which each node has radial basis function such as Gaussian) is the most frequently model that is used in neuro-fuzzy systems. Each fuzzy system is implemented by applying two methods that are Mamdani and Takagi–Sugeno–Kang models. In this study, the proposed model is developed based on Takagi–Sugeno–Kang method that is involved in framework of adaptive system. This ANFIS model is optimized with a partial swarm optimization (PSO) algorithm. For this purpose, two main parameters of each ANFIS model that are antecedent and consequent parameters (these parameters connect the fuzzy rules to each other) are optimized with PSO algorithm. A basic ANFIS structure is shown in Fig. 6. This structure contains five layers with two inputs and one output.

The structure of ANFIS model is described as follows:

Layer 1

This layer is called fuzzification layer and the signal that is achieved from each node is transferred to the other layer. Outputs of the cells (O_i^1) are described by Eq. (4) [48].

$$O_i^1 = \mu_{A_i}(x), \qquad i = 1,2 \tag{4}$$

In which i, A_i and μ_{A_i} are the input to node i, linguistic variable associated with this node function and membership function of A_i, respectively. In the most ANFIS models μ_{A_i} is selected as:

$$\mu_{A_i}(x) = exp\left\{-\left(\frac{x-c_i}{a_i}\right)^2\right\} \tag{5}$$

In which x is the input and $\{a_i,c_i\}$ are premise parameters.

Layer 2

This layer is called the rule layer that is obtained with the membership degrees (each node output represents the firing strength of a fuzzy rule).

$$O_2^i = w_i = \mu_{A_i}(x).\ \mu_{B_i}(y), \qquad i = 1,2 \tag{6}$$

Layer 3

This layer is called the normalization layer that every node in this layer is a fixed node labeled N. The ith node calculates the ratio of the rule's firing strength to the sum of all rules' firing strengths:

$$O_3^i = \overline{w}_i = \frac{w_i}{w_1 + w_2}, \qquad i = 1,2 \tag{7}$$

Layer 4

This layer is the defuzzification layer in which output value for each rule is calculated from the value of the previous layer.

$$O_4^i = \overline{w}_i f_i = \overline{w}_i(p_i x + q_i y + r_i), \qquad i = 1,2 \tag{8}$$

In which $\overline{w}_i$ is a normalized firing strength from layer 3 and $\{p_i,q_i,r_i\}$ are the consequent parameters.

Layer 5

The last layer is the sum layer. The output of ANFIS model is obtained by collecting the output values of each rule that are obtained from the defuzzification layer.

$$O_5^i = overall\ output = \sum_i \overline{w}_i f_i = \frac{\sum_i w_i f_i}{\sum_i w_i}, \qquad i = 1,2 \tag{9}$$

Particle swarm optimization (PSO)

Partial swarm optimization (PSO) has been introduced by Russell Eberhart and James Kennedy in 1995. It inspired by the flocking and schooling patterns of birds and fish [49]. Population of particles is used by every PSO algorithm. In this population, each particle is interconnected to other particles (this interconnection is called the neighborhood topology). It is noteworthy that here neighborhood means a communication structure. A so-called change rule is needed to use these particles in order to explore the search space. Actually, the particles are

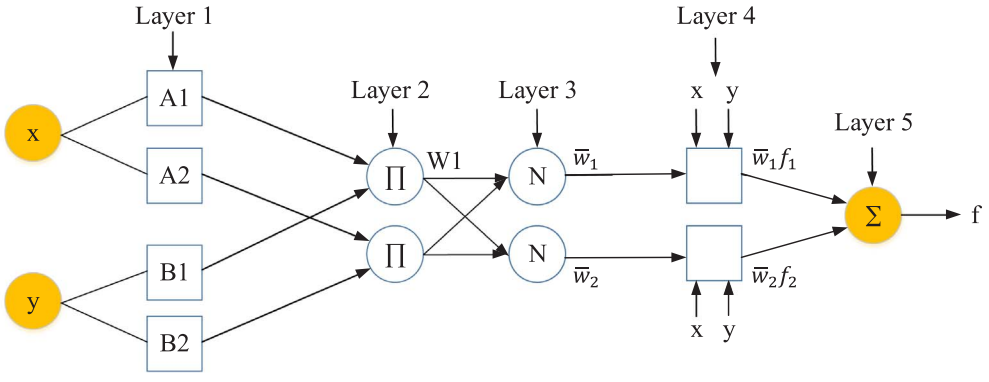

Fig. 6. ANFIS structure.

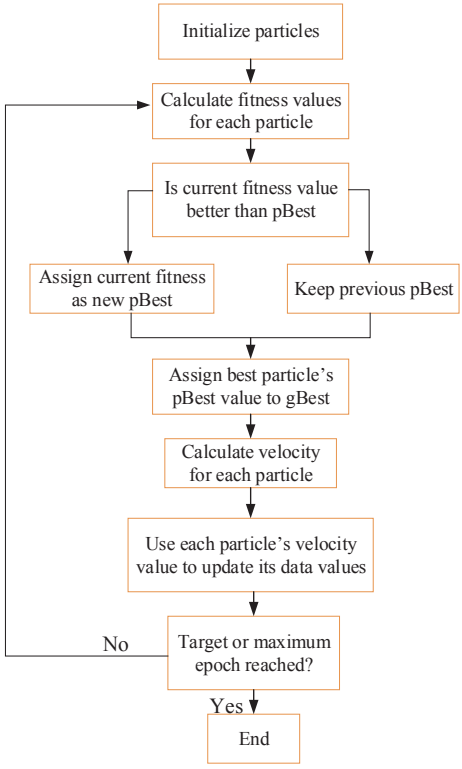

Fig. 7. Design structure of the PSO algorithm.

moved by the rule via the search space at given moment *t* that this time is dependent on its position at moment *t-1* also the position of its prior best location. This process is the cognitive aspect of the PSO. Interaction rule introduces the social aspect of a PSO. A position of particle is dependent on its own best position in history and as well as the best position in history of its neighbors. A flow diagram of PSO algorithm is presented in Fig. 7. The algorithm follows three main stages that are described as follows:

1. The target (or conditions) of the problem that is defined for the PSO algorithm.
2. Global best (gBest) that this variable for each PSO algorithm defines which particle's data is closer to the target.
3. Stop condition that determines when the algorithm should be stop.

Also, each particle contains:

1. $\vec{x}_i$; this vector shows the current position in the search space for the particle *i*.
2. $\vec{p}_i$; the best position in history of particle *i* is defined by this vector $\vec{v}_i$; the particle's velocity of the particle *i*.
3. $pBest_i$; this parameter indicates the quality of solution of the best position of particle *i*.

Training ANFIS using PSO algorithm

The ANFIS parameters are updated with the PSO algorithm. ANFIS has two main parameters that are premise and consequent parameters. These parameters should be updated with the optimization algorithm. The premise parameters are $\{a_i,c_i\}$ that belong to *Gaussian* membership function and are given in Eq. (5). The total number of these parameters is equal to the sum of the parameters in all membership functions. Consequent parameters are $\{p_i,q_i,r_i\}$ and use in defuzzification layer and are given in Eq. (8).

Energy and exergy analysis of wind energy

Energy and exergy analysis for the wind energy in the case study zone is done in this section. For this purpose, a WT (Enercone-E44, 900 kW) is selected that the technical specification of it is shown in Table 1.

Energy analysis

The amount of the energy balance for a WT is presented by the following equation:

$$ke_1 = w_{out} + ke_2 \tag{10}$$

where ke is the kinetic energy of the wind-flow and w_{out} is the output work that extracted by rotor blades. Kinetic energy of wind is defined as:

$$ke = \frac{1}{2}\rho A t v^3 \tag{11}$$

And then, the value of power is:

$$P = \frac{1}{2}\rho A v^3 \tag{12}$$

Based on the law of Betz [50] the theoretical maximum power efficiency of any design of WT is $Cp_{max} = 0.59$. Since WT cannot work in Cp_{max}, the actual power produced by each WT is defined by:

$$P_m = \frac{1}{2}\rho Cp A v^3 \tag{13}$$

Now that the mechanical power of the rotor is known, it must be determined how much of this power makes it to the electrical grid. A simplified overview of the energy transfer from wind to the electrical grid is shown in Fig. 8. It is necessary to calculate the efficiencies of the gearbox, generator and power electronics for each WT system. The received power to the electrical grid is obtained:

$$P_e = \eta_{gb}\,\eta_{gn}\,\eta_p P_m \tag{14}$$

In this study, the efficiencies of the gearbox, generator and power electronics device were assumed to be $\eta_{gb} = 0.95$, $\eta_{gn} = 0.97$ and $\eta_p = 0.98$, respectively [35].

Finally, energy efficiency of the WT system is:

$$\eta = \frac{P_e}{P} \tag{15}$$

Exergy analysis

By applying the second law of thermodynamics with the mass conservation and energy principals, exergy analysis will be introduced

Table 1
Technical specifications of WT (E-44).

Rated power:	900 kW
Rotor diameter:	44 m
Hub height in meter:	45/55
WEC concept:	Gearless, variable speed, single blade adjustment
Rotor type:	Upwind rotor with active pitch control
Rotational direction:	Clockwise
No. of blades:	3
Rotational speed:	Variable, 16–34.5 rpm

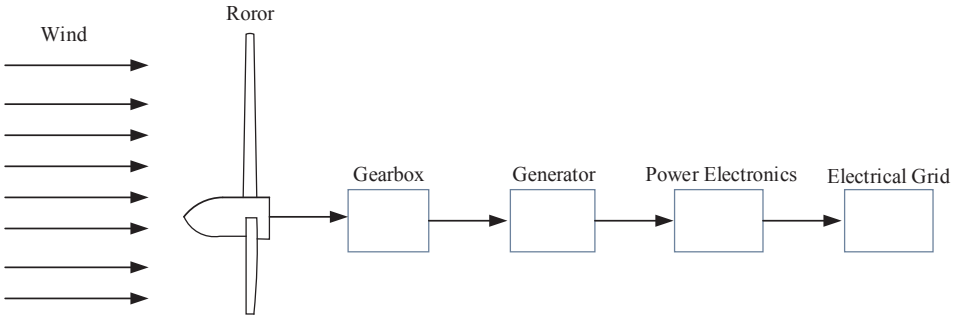

Fig. 8. Energy transfer from wind to electrical grid.

in the WT. The exergy analysis for the WT is presented by the following equation:

$$\dot{E}x_{flow_1} = \dot{W}_{out} + \dot{E}x_{flow_2} + \dot{E}x_{dest} \tag{16}$$

where $\dot{E}x_{flow_1}$, $\dot{W}_{out}$ and $\dot{E}x_{dest}$ are the exergy rate of the flow in the inlet of the WT, the rate of the output work and the rate of the exergy destruction of the WT, respectively. The exergy of flow is given by:

$$Ex_{flow} = (Ex_k + Ex_p + \Delta H - T_{amb}\Delta S) + Ex_{ch} \tag{17}$$

where Ex_k, Ex_p, ΔH, T_{amb}, ΔS and Ex_{ch} are kinetic energy, potential energy, enthalpy difference, ambient temperature, entropy difference and chemical energy. Whereas, there is no difference in the high of the WT so the value of the potential energy is supposed to be zero. The value of the kinetic exergy is defined by the generated electricity which is:

$$Ex_k = E_{generated} \tag{18}$$

And the enthalpy difference is:

$$\Delta H = \dot{m}cp_a(T_2 - T_1) \tag{19}$$

In which $\dot{m}$ is the mass flow rate of the air, cp_a is the specific heat of the air, T_1 and T_2 are the wind chill temperature at the inlet and outlet of the WT respectively and is given by the following equation [51].

$$T_{i,wind-chi} = 13.12 + 0.6215T_{amb} - 11.37v_i^{0.16} + 0.3965T_{amb}v_i^{0.16} \tag{20}$$

The wind speed is in *km/hr* at 10-meter elevation and the value of the will be obtained in °C. The amount of the wind speed after the WT is defined by [51]:

$$v_2 = \sqrt[3]{\frac{2(E_{potential} - E_{generated})}{\rho A t}} \tag{21}$$

Physical exergy of the air is given by Eq. (22) that was developed by Ref. [52].

$$Ex_{ph} = (cp_a + \omega cp_v)T_0\left[\frac{T}{T_0} - 1 - ln\left(\frac{T}{T_0}\right)\right] + (1 + 1.6078\omega)RT_0 ln\left(\frac{P}{P_0}\right) \tag{22}$$

where cp_a is the air specific heat, cp_v is the vapor specific heat, ω is humidity ratio, R is the gas constant and P_0 is the reference pressure. Also, the pressure in the inlet and outlet of the WT is obtained by:

$$P_i = P_a \pm \frac{\rho}{2}v_i^2 \tag{23}$$

Table 2
Prediction of the wind speed and its direction using MLFFNN.

Wind speed prediction for January with 10-min interval						
	Algorithm	RMSE(m/s)	R	Computation time	Epoch	MSE(m/s)
LM	trainlm	0.3226	0.9828	0:02:03	423	0.1041
BFG	trainbfg	0.4689	0.9634	0:00:41	342	0.2199
RP	trainrp	0.7169	0.9124	0:00:07	361	0.5140
SCG	trainscg	0.8361	0.8786	0:00:04	115	0.6991
CGB	traincgb	0.7705	0.8980	0:00:10	132	0.5937
CGF	traincgf	0.7634	0.8999	0:00:16	202	0.5828
CGP	traincgp	0.7888	0.8930	0:00:13	163	0.6212
OSS	trainoss	0.7730	0.8973	0:00:17	191	0.5976
BR	trainbr	0.2958	0.9856	0:05:13	1059	0.0875
Wind direction prediction for January with 10-min interval						
	Algorithm	RMSE(°)	R	Computation time	Epoch	MSE(°)
LM	trainlm	25.954	0.9791	0:02:39	214	673.644
BFG	trainbfg	69.372	0.8397	0:50:34	10,000	4812.477
RP	trainrp	66.087	0.8557	0:00:18	459	4367.534
SCG	trainscg	65.027	0.8595	0:00:24	322	4260.725
CGB	traincgb	72.749	0.8218	0:00:24	142	5292.431
CGF	traincgf	76.359	0.8015	0:00:24	139	5830.768
CGP	traincgp	72.556	0.8229	0:00:34	199	5264.469
OSS	trainoss	80.573	0.7759	0:00:48	153	6492.079
BR	trainbr	30.306	0.9714	0:06:28	488	918.468

The chemical exergy of the WT which is defined by Eq. (24).

$$Ex_{ch} = RT_0[(1 + 1.6078\omega)ln[(1 + 1.6078\omega_0)/(1 + 1.6078\omega)] + 1 + 1.6078\omega ln(\omega/\omega_0)] \quad (24)$$

Also, heat loss of the WT is:

$$\dot{Q}_{loss} = \dot{m}_a cp_a(T_2 - T_1) \quad (25)$$

And entropy generation is calculated by the following equation.

$$\dot{I} = T_0\left(cpln\left(\frac{T_2}{T_1}\right) - Rln\left(\frac{P_2}{P_1}\right) - \frac{\dot{m}cp(T_{amb} - T_{ave})}{T_{amb}}\right) \quad (26)$$

The specific exergy destruction can be defined by:

$$Ex_{des} = \frac{T_0 \Delta S}{\rho A v} \quad (27)$$

And the exergy efficiency of the WT is given by the following equation.

$$\psi = \frac{\dot{w}_{out}}{\dot{E}x_{flow}} \quad (28)$$

Result and discussion

Wind power generation depends on wind speed, thus, wind speed prediction becomes increasingly important for modern wind farm management and supply-demand balancing in the smart grid. However, wind speed is generally very difficult to estimate, due to its non-stationary and intermittent nature. There are a number of traditional methods for prediction of wind speed that most of them are involve the statistical analysis of the data. In dynamic systems, these models cannot predict the targets with high accuracy. Hence, authors proposed machine learning algorithms to predict the targets in these dynamic systems. The network was developed with temperature, pressure, local time and relative humidity as input variables and the targets are wind speed, wind direction and output power of a WT. To evaluate the performance of the models three statistical parameters that are root mean square error (RMSE), correlation coefficient (R) and mean square error (MSE) are used. These parameters are described in Appendix A. During data training, a smaller error between the outputs and targets can be found. When the new data are interred to the neural network, it can be achieved high error in outputs that this situation is called overfitting. In this study to avoid overfitting problem, the data were divided into two sections as 70% training datasets and 30% as testing datasets.

MLFFNN model

ANN is a promising method for adaptive the prediction of targets. Table 2 illustrates prediction of the wind speed and its direction using MLFFNN. To obtain the best performance nine data training algorithms were applied. The results show in January for 10-min interval data, BR and LM algorithms have the maximum R and minimum RMSE and MSE. But the computation time and number of iteration for LM are lower than BR algorithm. Also, BFG algorithm reports an accuracy above 96%. RP and SCG algorithms are faster than others training algorithms. It is observed that prediction wind direction is harder than wind speed for the network. The designed network needs much the computation time to predict the wind direction. Fig. 9 demonstrates the training phase of the model to predict wind speed for 24 h. Moreover, for prediction of wind direction the training phase of the model with different data training algorithms are shown in Fig. 10. Both figures illustrate that LM and BR can successfully train the models. Reaching good forecasting accuracy for MLFFNN also depends on the suitable number of neurons in the hidden layer. The smallest errors of statistical indices were obtained for 75 neurons in the hidden layer for wind speed prediction and 175 neurons for wind direction forecasting model.

Fig. 11 illustrates the testing phase of wind speed prediction for 24 h of January. This graph shows that the overfitting problem has considered for designing the network and the results with new data have an approximately similar trend with the data training process. For this prediction, LM, BFG and BR show satisfactory predicted wind speed data.

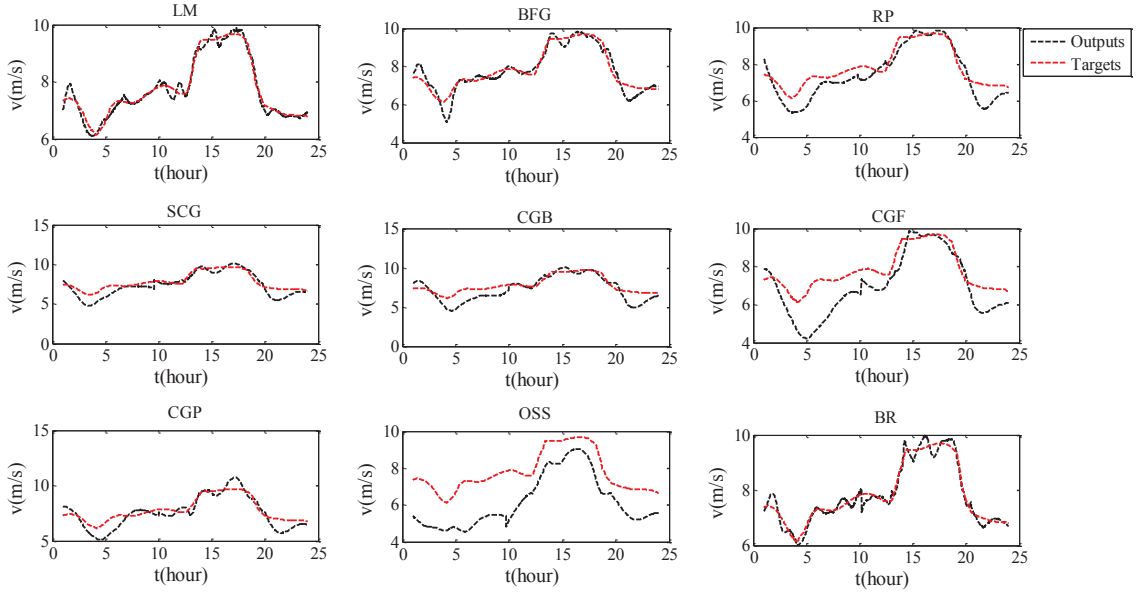

Fig. 9. Comparison of the different training algorithms for wind speed prediction for MLFFNN.

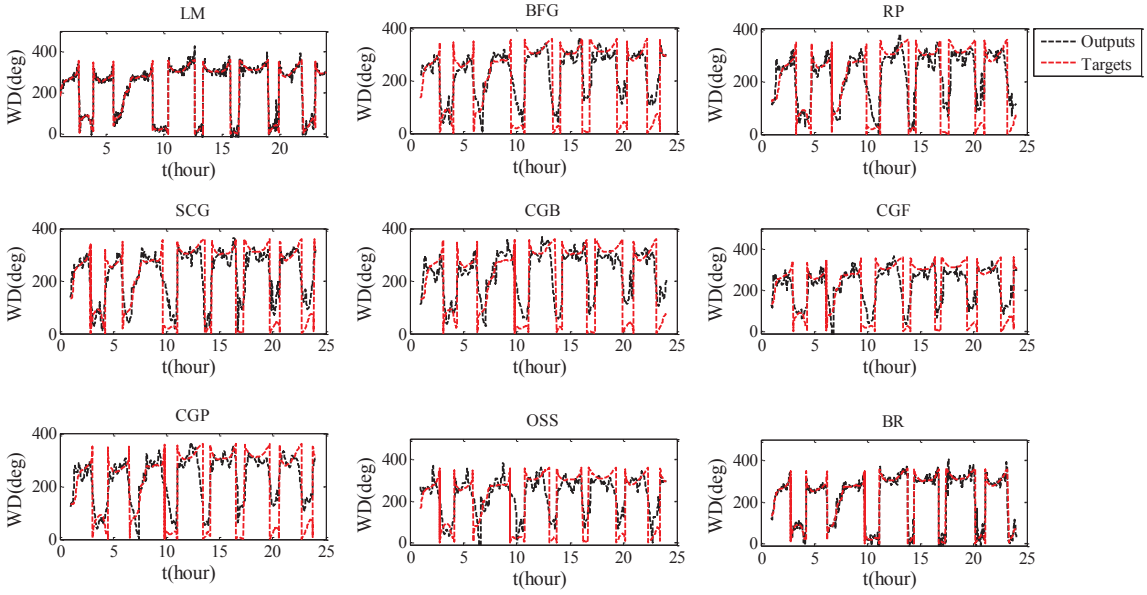

Fig. 10. Comparison of training algorithms for prediction of wind direction for MLFFNN.

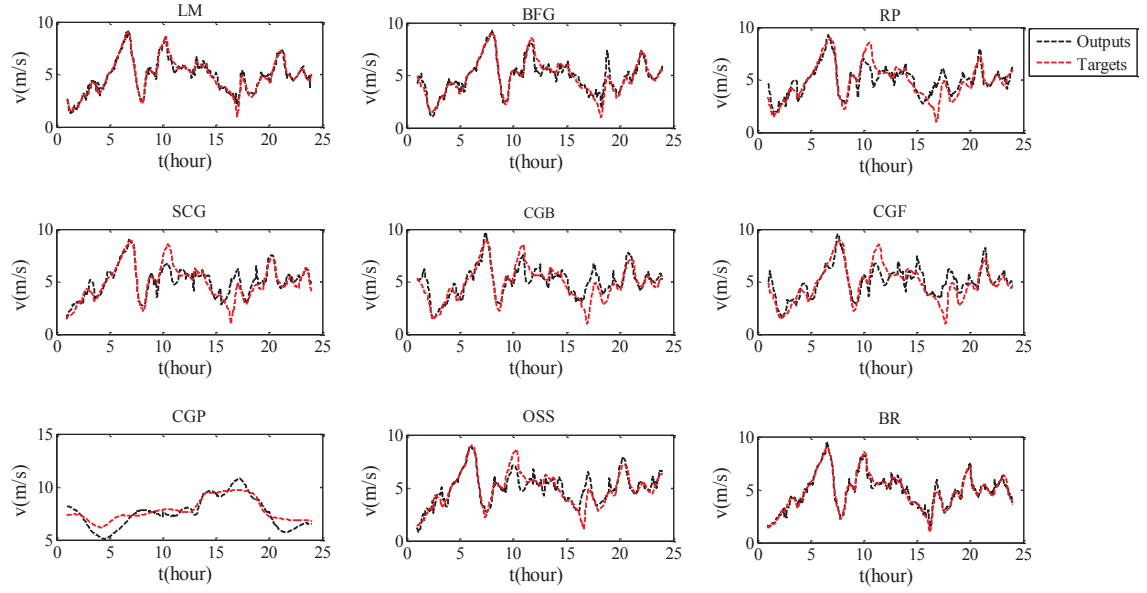

Fig. 11. Test data of MLFFNN for 24 h.

Table 3
Design parameters of SVR-RBF for wind speed forecasting (10-min interval).

Model		RMSE (m/s)	R	MSE (m/s)
1	$\varepsilon = 1, \sigma = 1, C = 1$	0.8647	0.9286	0.7478
2	$\varepsilon = 0.5, \sigma = 1, C = 100$	0.4504	0.9811	0.0202
3	$\varepsilon = 0.02, \sigma = 1, C = 1000$	0.0191	0.9999	0.0003
4	$\varepsilon = 0.02, \sigma = 0.5, C = 1000$	0.0184	0.9999	0.0003

SVR-RBF model

Support vector regression was developed to predict the targets. This model was implemented based on RBF as a kernel function. Hence, this model was called SVR-RBF. This model was adjusted with three user-defined parameters. These parameters are ε (is the error defined by the user), σ (is a predefined value which controls the width of the Gaussian function) and C (cost parameter C handles the trade-off between errors in the predictions (first term) and complexity (second term)). Different values of these parameters are reported in Table 3. The best performance of the model was achieved for Model-4 of SVR in terms of RMSE = 0.0184 (m/s), R = 0.9999 and MSE = 0.0003 (m/s).

Also, Fig. 12 demonstrates the prediction of wind direction in six different values of user-determined parameters. The performance of the model with different values of ε, σ and C is shown in this graph in which Fig. 13(f) shows the best performance by ε = 0.5, σ = 1 and C = 1000.

ANFIS-PSO model

The developed ANFIS model is called ANFIS-FCM that uses fuzzy c-means clustering to generate a fuzzy inference system. Obtaining good

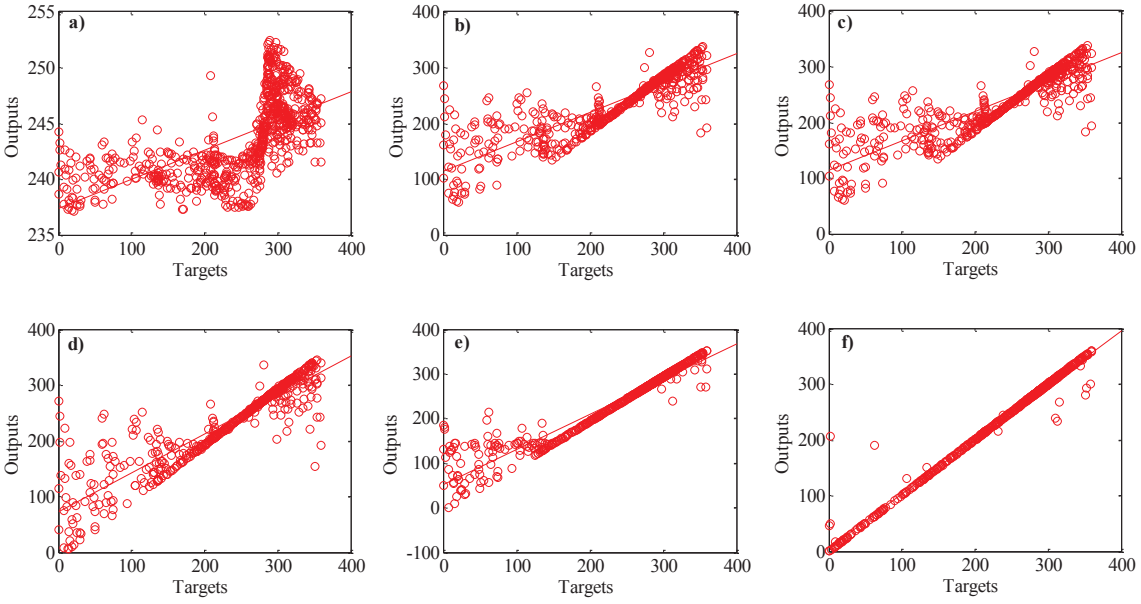

Fig. 12. SVR-RBF with different user-determined parameters: (a), ε = 1, σ = 1, C = 1, (b), ε = 1, σ = 1, C = 30, (c), ε = 0.5, σ = 1, C = 30, (d), ε = 0.5, σ = 1, C = 50, (e), ε = 0.02, σ = 0.5, C = 100, (f), ε = 0.5, σ = 1, C = 1000.

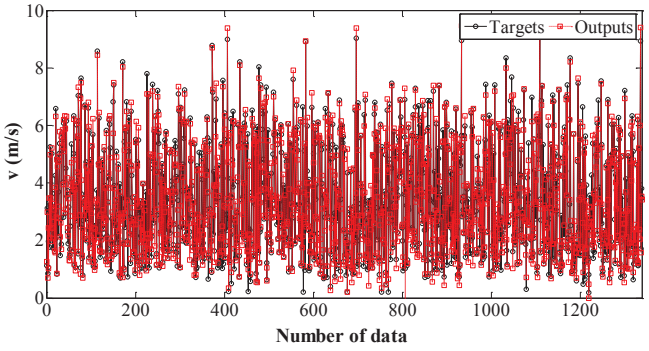

Fig. 13. Actual and predicted wind speed data for 10-min interval using ANFIS-PSO.

Table 4
A comparison between ANFIS and ANFIS-PSO models for 5-min interval of wind speed data.

	RMSE (m/s)		R		MSE (m/s)	
	Train	Test	Train	Test	Train	Test
ANFIS	0.8466	0.8420	0.8898	0.8888	0.7167	0.7090
ANFIS-PSO	0.1700	0.2321	0.9958	0.9922	0.0289	0.0538

accuracy using ANFIS can be achieved by adjusting the suitable number of clusters for the model. It depends on the number of data that are considered for training model. A large number of trials were done to obtain the suitable number of clusters for the model. Finally, the model was developed with 300 clusters in which the maximum accuracy for the model obtained. Generally, for this specific problem, as can be seen in Table 4, the ANFIS model cannot predict the target with high accuracy. Hence, a PSO algorithm was considered to optimize the ANFIS parameters. The PSO parameters were selected as follows: the size of population is 200, the maximum iteration is 1500, C_1 = 1 (personal learning coefficient), C_2 = 2 (global learning coefficient) and Inertia weight was considered as 1. The correlation coefficient, which indicates the goodness of fit of the model, for the ANFIS model is reported to be 0.8991 and 0.8995 for the training and testing datasets, respectively. The PSO algorithm can successfully improve the performance of the ANFIS model and the novel method outperforms the ANFIS model.

Fig. 13 demonstrates the prediction of wind speed with the ANFIS-PSO model agrees well with the target data and the magnitude of the disagreement between the actual and predicted data is small.

Table 5
A comparison between the developed models to predict wind speed data.

	RMSE(m/s)		R		MSE(m/s)	
	Train	Test	Train	Test	Train	Test
5-min interval						
MLFFNN	0.2143	0.2450	0.9933	0.99108	0.0459	0.0600
SVR-RBF	0.0206	0.0213	0.9999	0.9999	4.23E−04	4.53E−04
ANFIS-PSO	0.1700	0.2321	0.9958	0.9922	0.0289	0.0538
10-min interval						
MLFFNN	0.1373	0.2216	0.9972	0.9924	0.0189	0.0491
SVR-RBF	0.0439	0.0526	0.9997	0.9996	0.0019	0.0028
ANFIS-PSO	0.1819	0.3549	0.9951	0.9824	0.0331	0.1259
30-min interval						
MLFFNN	0.2053	0.7437	0.9940	0.9123	0.0421	0.5532
SVR-RBF	0.1800	0.1808	0.9951	0.9957	0.0324	0.0327
ANFIS-PSO	0.4566	0.7965	0.9686	0.9103	0.2085	0.6344
1-h interval						
MLFFNN	0.3589	0.9382	0.9831	0.8631	0.1288	0.8803
SVR-RBF	0.3669	0.3651	0.9824	0.9796	0.1346	0.1333
ANFIS-PSO	0.590	1.0312	0.9474	0.8534	0.3481	1.0634

Models comparison

The developed models were applied to predict the targets. Actually, we proposed a network with pressure, temperature, local time and

Table 6
A comparison between the developed models to predict wind direction data.

	RMSE(°)		R		MSE(°)	
	Train	Test	Train	Test	Train	Test
5-min interval						
MLFFNN	15.922	23.572	0.9822	0.9612	253.528	555.67
SVR-RBF	8.1018	14.2148	0.9945	0.9918	65.638	202.061
ANFIS-PSO	16.2761	23.7135	0.9817	0.9612	264.910	562.3316
10-min interval						
MLFFNN	20.498	29.110	0.9710	0.9373	420.204	847.441
SVR-RBF	23.306	25.907	0.9592	0.9379	640.394	671.173
ANFIS-PSO	22.7428	0.37068	0.9638	0.9074	517.2342	1374.0433
30-min interval						
MLFFNN	32.212	54.418	0.9243	0.8007	1037.616	2961.400
SVR-RBF	8.5732	8.4891	0.9955	0.9927	73.5002	72.0641
ANFIS-PSO	44.189	61.2601	0.8570	0.7201	1952.6645	3752.7941
1-h interval						
MLFFNN	33.459	69.933	0.9236	0.6284	1119.529	4890.751
SVR-RBF	13.9711	19.4433	0.9824	0.9765	195.1904	378.0410
ANFIS-PSO	40.255	87.9549	0.8784	0.5368	1620.4624	7736.056

relative humidity as inputs variables that can predict wind speed, wind direction and output power of the considered WT in the case study region. Four samples of datasets were considered to evaluate the proposed models. Wind speed data with 5-min interval (8928 data), 10-min interval (4464 data), 30-min interval (1488) and 1-h interval (744 data) for June 2017 were selected for this investigation. Comparison of the models for RMSE, R and MSE values can be observed clearly in Table 5. The lowest statistical errors and the highest correlation coefficient were obtained with the SVR-RBF model for all time intervals. The obtained correlation coefficient of the MLFFNN and ANFIS-PSO models (for 5-min and 10-min intervals) illustrate the predicted wind speed (outputs) agrees well with the actual data (targets) and the magnitude of the disagreement between the outputs and targets is small. For 30-min and 1-h intervals, the SVR-RBF outperforms the MLFFNN and ANFIS-PSO models in terms of RMSE, R and MSE. Moreover, the MLFFNN and ANFIS-PSO models approximately have the same ability to predict the wind speed data.

Also, the performances of the MLFFNN, SVR-RBF and ANFIS-PSO models for wind direction forecasting are compared using a comprehensive wind direction samples. For the 5-min interval, the correlation coefficient is 0.9612 for MLFFNN and ANFIS-PSO and is 0.9918 for SVR-RBF. As expected, the SVR-RBF is more accurate than MLFFNN and ANFIS-PSO models. Generally, the developed models have lower performance for prediction of wind direction compared to wind speed forecasting. This investigation is shown in Table 6.

Wind turbine

In this section, energy and exergy analysis for evaluating the potential of power energy in the case study zone have been conducted. For this investigation, a WT (E-44, 900 kW) was considered. Fig. 14 demonstrates the curves of the power coefficient and the produced power of the WT in this region. The curve of power coefficient (Fig. 14(a)) can be divided into three distinct sections according to the wind speed: from 0 to 2 m/s that the power coefficient is zero; from 2 to 7 m/s in which power coefficient increases gradually and reaches the maximum value in 7 m/s; after that there is a moderate decrease between 7 and 14 m/s. Also, analysis of the generated electric power of the WT versus wind speed (Fig. 14(b)) illustrates that from 0 to 4 (m/s) cannot see an impressive generated power. Also, between 4 and 14 m/s the trend is obviously upwards and reaches to approximately 700 kW. Fig. 15 demonstrates the generated power of the WT for one month (January), one day (March 3rd) and one year (2016) in Bushehr. The wind speed and its direction are always changing thus the produced power has different value and it changes from 0 to around 700 kW, but for 3rd March is less than the maximum value and it varies between 0 and around 100 kW. It should be noted that the curves in Fig. 14 were given based on R-Squared. This parameter is a statistical measure of how close the data are to the fitted regression line.

Fig. 15 illustrated the output power of the WT for every hour of the day in an annual period. The developed models with the considered inputs are applied to predict the output power of the WT (E-44). Table 7 shows the performances of this prediction. The SVR-RBF performs better than the MLFFNN and ANFIS-PSO models. Also, Fig. 16 demonstrates the testing phase of the SVR-RBF model to predict the output power of the WT.

WT blades capture a fraction of the kinetic energy from the air passing turbine blades and convert it from mechanical to the electrical energy. Fig. 17 illustrates the energy efficiency of the WT for December and April in the case study zone that is obtained from Eqs. (10)–(15) and by considering the efficiencies of the gearbox, generator, and power electronics device. The results show that the energy efficiency changes from 0 to 0.5 and the average of it, is approximately 32%. Also, the graph illustrates that the value of the energy efficiency for December is more than April and in the most of the time is around 40%.

Exergy analysis based on the second law of the thermodynamics can

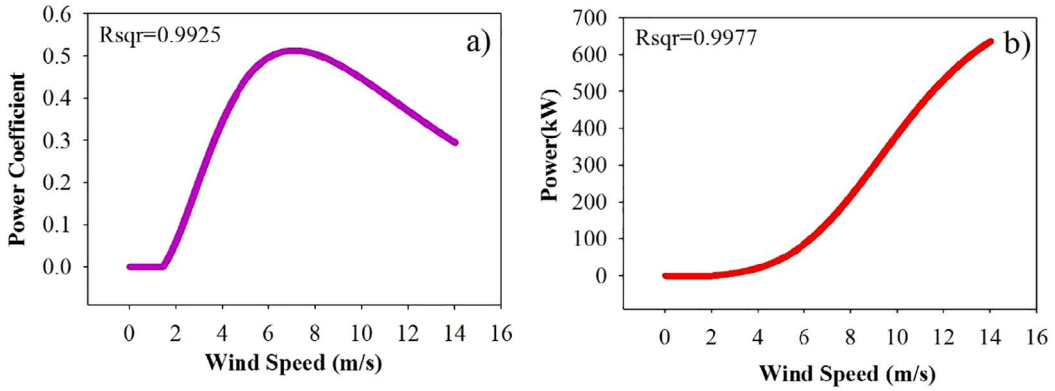

Fig. 14. Power coefficient and produced electric power (kW) versus wind speed (m/s) for WT.

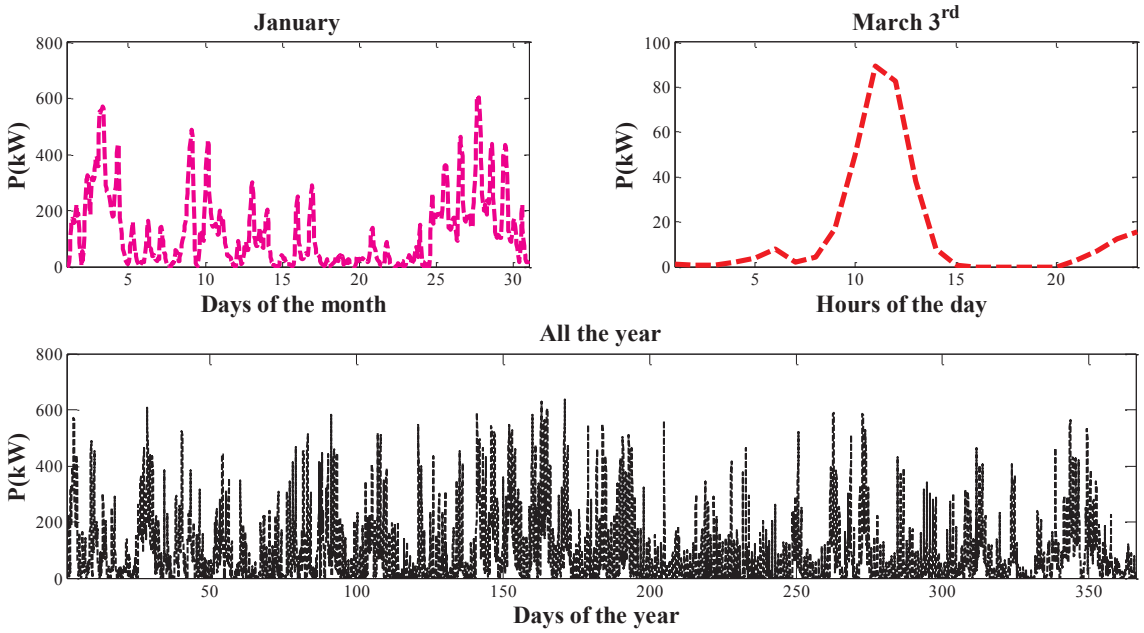

Fig. 15. Electric power produced (kW) by the WT for one month, one day and one year.

Table 7
Prediction of output power of the WT (E-44) using the forecasting models.

	RMSE (kW)		R		MSE (kW)	
	Train	Test	Train	Test	Train	Test
MLFFNN	49.6508	97.3696	0.9368	0.8121	2465.2022	9480.8466
SVR-RBF	7.2940	11.0351	0.9982	0.9970	53.2019	121.7734
ANFIS-PSO	69.8736	93.511	0.8351	0.7578	4882.3225	8744.3023

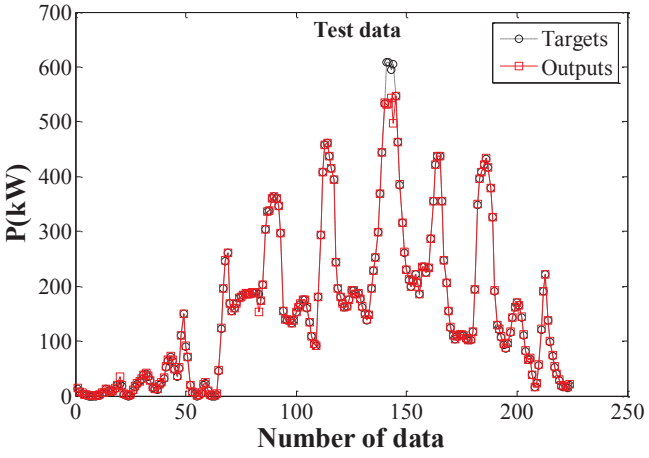

Fig. 16. Testing phase of the SVR-RBF model to predict the output power of the WT.

support to create the strategies and management for more economical and effective use of energy sources and is utilized to study wind energy system. Exergy analysis gives better comprehension of performance than the energy efficiency [53]. Because it demonstrates the external losses and internal irreversibility that should be dealing with to improve efficiency. Eqs. (16)–(28) were used to calculate the exergy efficiency of the WT. Fig. 18 illustrates exergy analysis of the WT in the case study region. It is clear that inlet and outlet exergy of the system is mainly attributed to the wind speed. It is seen that produced exergy efficiency has been changed between 0 and 37% at different measured wind speed. Also, the average exergy efficiency for the WT is 25.41% over an annual period.

In February and August, the value of the exergy efficiency is shown in Fig. 19. This figure indicates that the amount of the exergy efficiency for February is between 0 and 0.35. Exergy efficiency in February in all time of the day is around 30% that this value for August is only between 9:00 and 15:00. Exergy efficiency changes in different wind speed also meteorological data like pressure and relative humidity can change the value of this parameter [37].

Conclusion

Although Iran is among the countries with the huge reserves of fossil fuels and non-renewable sources of energy such as oil and gas, it benefits a remarkable potential of renewable energies such as the wind, solar, biomass and geothermal. The wind turbine system is one of the most competitive sources in the field of renewable energy technologies. Despite several studies which investigated wind energy in different worldwide regions, different patterns of power produced from wind energy have led to the fact that this research is being continued in wind energy systems. This study has led to conclusions in the following:

Three methods of machine learning algorithms were developed to predict the wind speed, wind direction and output power of the WT in Bushehr, located in the south of Iran. Pressure, temperature, local time and relative humidity of the region were considered to be the input variables. The first model was MLFFNN that was trained with nine data training algorithms. The LM and BR algorithms have shown the minimum errors between the actual and predicted data. The second model was SVR with RBF as kernel function. This model was adjusted with three different used-defined parameters that the best performance of the model was obtained by $\varepsilon = 0.5$, $\sigma = 1$ and $C = 1000$. The third

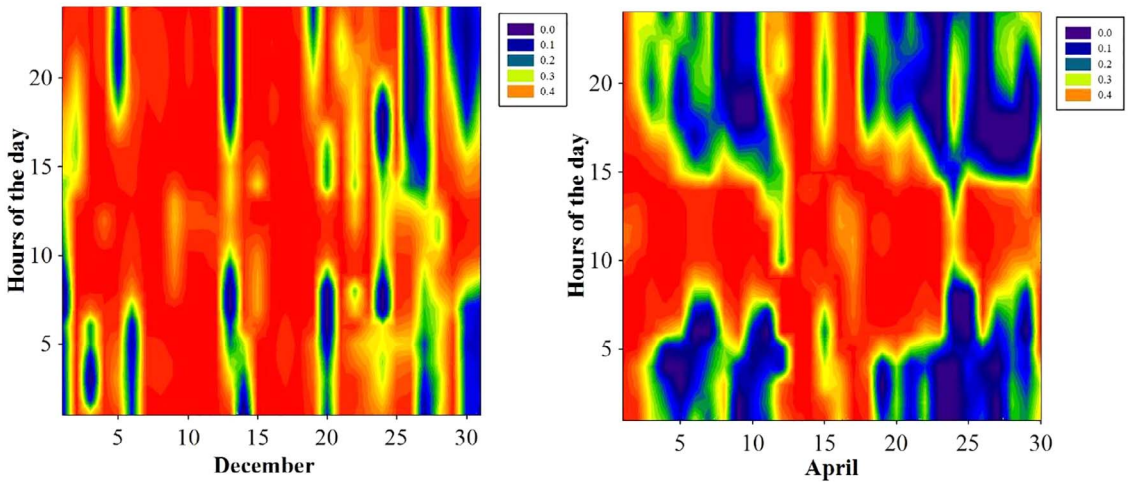

Fig. 17. Energy efficiency of the WT in December and April.

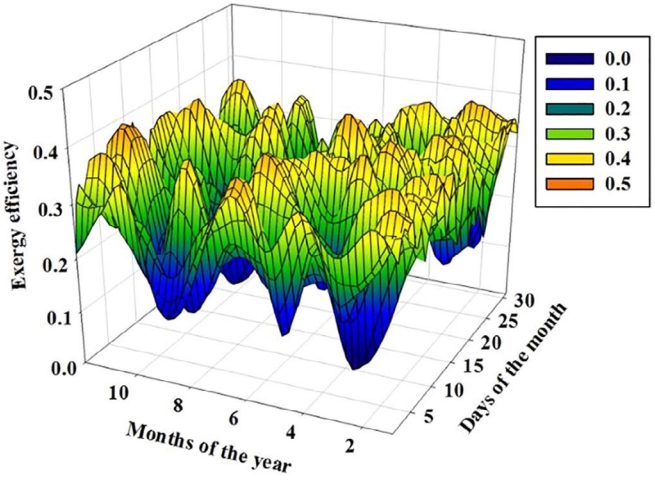

Fig. 18. Exergy efficiency of the WT for the study zone.

method was ANFIS that was optimized with a PSO algorithm. Forecasting models were compared with 5-min, 10-min, 30-min and 1-h intervals of wind speed and its direction. For 5-min and 10-min intervals of wind speed data, the predicted values were found to be in excellent agreement with the actual data for three developed models. For other time intervals, the SVR-RBF model performs better than the MLFFNN and ANFIS-PSO in terms of R, MSE and MSE. For wind direction prediction, the developed models have shown lower performance compared to wind speed prediction.

Wind turbine (E-44, 900 kW) was considered to investigate the wind energy in the case study zone. Developed models were applied to predict the output power of the WT. As expected, the SVR-RBF model outperformed the MLFFNN and ANFIS-PSO models. Also, in order to investigate the wind energy potential of the region, energy and exergy analysis of the WT were done. Despite the energy efficiency for some days is close to 50%, the average energy efficiency in this zone for the WT was reported to be 31.46%. Exergy analysis using the second law of thermodynamics for evaluating the quality of energy was done in this station. Exergy efficiency of the wind turbine was changed between 0 and 37% and the average value of it was obtained to be 25.41%.

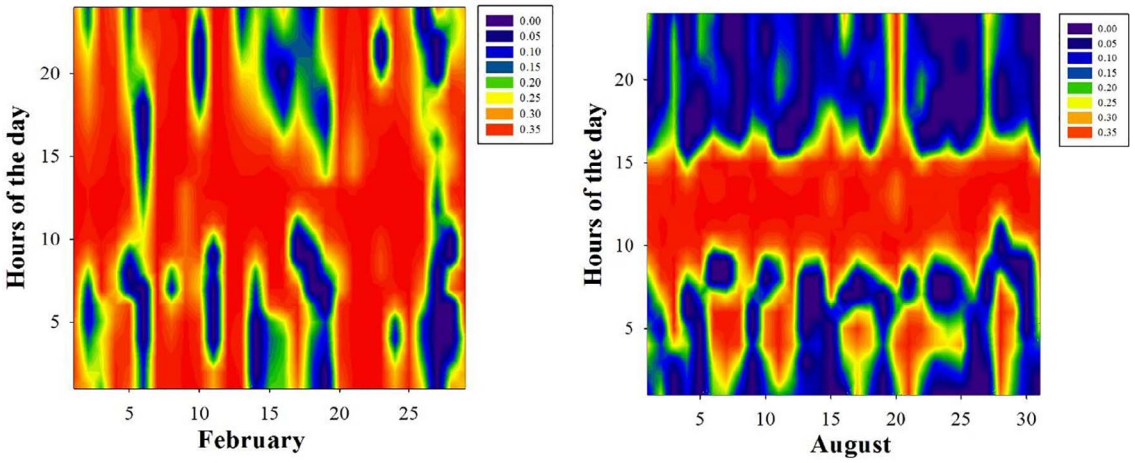

Fig. 19. Exergy efficiency of the WT in February and August for the study zone.

Appendix A

Performance evaluation measures

To evaluate the performance of the developed models mean square error (MSE), root mean square error (RMSE) and regression coefficient (R) were used that are given by the following equations:

$$RMSE = \sqrt{\frac{1}{n}\sum_{i=1}^{n}(x_i - y_i)^2} \tag{A.1}$$

$$MSE = \frac{1}{n}\sum_{i=1}^{n}(x_i - y_i)^2 \tag{A.2}$$

$$R = \frac{\sum_{i=1}^{n}(x_i - \overline{x})(y_i - \overline{y})}{\sqrt{\sum_{i=1}^{n}(x_i - \overline{x})^2 \sum_{i=1}^{n}(y_i - \overline{y})^2}} \tag{A.3}$$

In which x_i, y_i, $\overline{x}$, $\overline{x}$ and n are observed value, predicted value, mean of observed data, mean of predicted data and number of data, respectively.

Appendix B

Lagrange multipliers

In Eq. (3) α_i, α_i^* indicate the Lagrange multipliers. They can be obtained by maximizing the dual function of Eq. (1) and then can be introduced by:

$$\max_{\alpha_i \alpha_i^*} \sum_{i=1}^{n} y_i(\alpha_i - \alpha_i^*) - \varepsilon \sum_{i=1}^{n} y_i(\alpha_i - \alpha_i^*) - \frac{1}{2}\sum_{i=1}^{n}\sum_{j=1}^{n}(\alpha_i - \alpha_i^*)(\alpha_j - \alpha_j^*)\langle x_i, x_j\rangle \tag{B.1}$$

$$s.t. \begin{cases} \sum_{i=1}^{n}(\alpha_i - \alpha_i^*) = 0 \\ 0 \leqslant \alpha_i \leqslant C \\ 0 \leqslant \alpha_i^* \leqslant C \\ i = 1,2,\ldots,n \end{cases} \tag{B.2}$$

In Eq. (3), only some $(\alpha_i - \alpha_i^*)$ are not equal to zero, which comes from the Karush-Kuhn-Tucker's conditions of solving a quadratic programming problem. The support vector itself refers to the approximation error of data point on non-zero coefficient equal or larger than ε. Because errors lower than ε are acceptable, the data from the training set inside the "ε-tube" do not contribute to the cost nor the solution of the problem.

Kernel trick

The key to non-linear extension of the SVR is the Eq. (B.1) and the existence of the so-called kernel trick. The dot product of $\langle x_i, x_j\rangle$ from the Eq. (B.1) becomes a kernel function $\langle \varnothing(x_i), \varnothing(x_j)\rangle = k(x_i, x_j)$ in the case of non-linearity. The function $\varnothing$: $R^d \rightarrow \mathcal{H}$ presents the idea of mapping the input space into a feature space with a higher dimension. The common kernel function that satisfy this issue are:

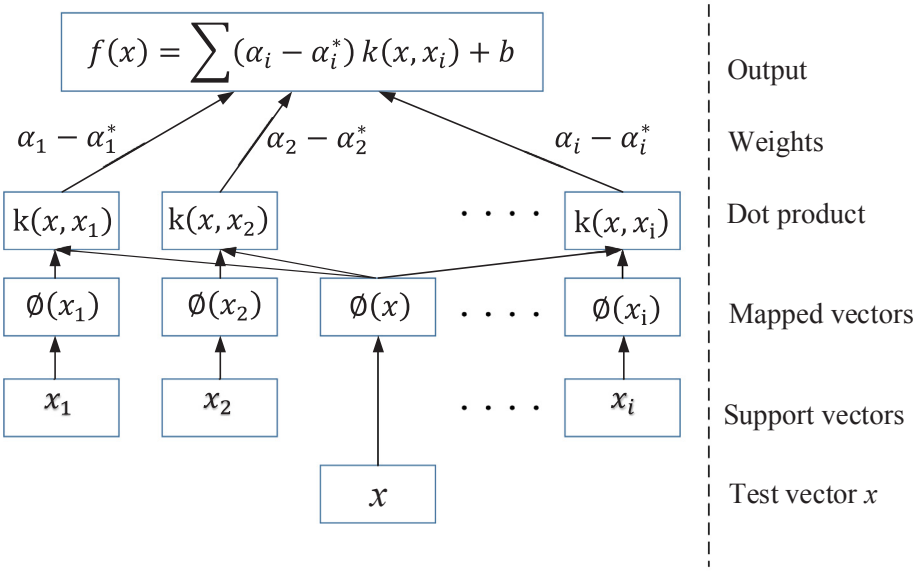

Fig. B.1. SVR architecture.

Linear kernel: $k_{lin}(x,x') = \langle x,x' \rangle$ (B.3)

Polynomial kernel: $\langle x,x' \rangle^p, p \in N$ (B.4)

Radial basis function (RBF): $K(x,x') = exp(-\sigma||x-x'||^2), \sigma \in R, \sigma > 0$ (B.5)

Fig. B.1 shows a SVRNN architecture based on Eq. (3) with considering the Karush-Kuhn-Tucker's conditions for solving a quadratic programming problem. The value of $(\alpha_i - \alpha_i^*)$ that are nonzero are support vectors, which are applied to obtain the decision function. It is important to find the optimum three user-determined parameters that are C, ε, and σ.

References

[1] Mohammadi K, Mostafaeipour A, Sabzpooshani M. Assessment of solar and wind energy potentials for three free economic and industrial zones of Iran. Energy 2014;67:117–28.
[2] Jiang Y, Huang G. Short-term wind speed prediction: hybrid of ensemble empirical mode decomposition, feature selection and error correction. Energy Convers Manage 2017;144:340–50.
[3] Ba Ü, Filik T. Wind speed prediction using artificial neural networks based on multiple local measurements in Eskisehir. Energy Proc 2017;107:264–9. September 2016.
[4] Kirbas I, Kerem A. Short-term wind speed prediction based on artificial neural network models. Meas Control 2016;49(6):183–90.
[5] Bilgili M, Sahin B, Yasar A. Application of artificial neural networks for the wind speed prediction of target station using reference stations data. Renew Energy 2007;32(14):2350–60.
[6] Ramasamy P, Chandel SS, Yadav AK. Wind speed prediction in the mountainous region of India using an artificial neural network model. Renew Energy 2015;80:338–47. March 2014.
[7] Paramasivan SK, Lopez D. Forecasting of wind speed using feature selection and neural networks. Int J Renew Energy Res 2016;6(3).
[8] Sreelakshmi K, Ramakanthkumar P. Neural networks for short term wind speed prediction. Int J Comput Electr Autom Control Inf Eng 2008;2(6):2019–23.
[9] Masrur H, Nimol M. Short term wind speed forecasting using artificial neural network: a case study. Int Conf Innov Sci Eng Technol 2016:0–4.
[10] Li G, Shi J. On comparing three artificial neural networks for wind speed forecasting. Appl Energy 2010;87(7):2313–20.
[11] Fazelpour F, Tarashkar N, Rosen MA. Short-term wind speed forecasting using artificial neural networks for Tehran, Iran. Int J Energy Environ Eng 2016.
[12] Doucoure B, Agbossou K, Cardenas A. Time series prediction using artificial wavelet neural network and multi-resolution analysis : application to wind speed data. Renew Energy 2016;92:202–11.
[13] Nogay HS. Application of artificial neural networks for short term wind speed forecasting in Mardin, Turkey. J Energy South Africa 2012;23(4):2–7.
[14] Jafarian M, Ranjbar AM. Fuzzy modeling techniques and artificial neural networks to estimate annual energy output of a wind turbine. Renew Energy 2014;35(9):2008–14.
[15] Asghar AB, Liu X. Estimation of wind turbine power coefficient by adaptive neuro-fuzzy methodology. Neurocomputing 2017;238:227–33.
[16] Chang GW, Lu HJ, Chang YR, Lee YD. An improved neural network-based approach for short-term wind speed and power forecast. Renew Energy 2017;105. p. 301e311 Contents.
[17] Filik ÜB, Filik T. Wind speed prediction using artificial neural networks based on multiple local measurements in eskisehir. Energy Procedia 2017;107(2016):264–9.
[18] Kumar G, Malik H. Generalized regression neural network based wind speed prediction model for western region of India. Procedia Comput Sci 2016;93:26–32.
[19] Mi X, Liu H, Li Y. Wind speed forecasting method using wavelet, extreme learning machine and outlier correction algorithm. Energy Convers Manage 2017;151:709–22.
[20] Kaplan O, Temiz M. A novel method based on Weibull distribution for short-term wind speed prediction. Int J Hydrogen Energy 2017;42(28):17793–800.
[21] Meng A, Ge J, Yin H, Chen S. Wind speed forecasting based on wavelet packet decomposition and artificial neural networks trained by crisscross optimization algorithm. Energy Convers Manage 2016;114:75–88.
[22] Santamaría-Bonfil G, Reyes-Ballesteros A, Gershenson C. Wind speed forecasting for wind farms: a method based on support vector regression. Renew Energy 2016;85:790–809.
[23] Schicker I, Papazek P, Kann A, Wang Y. Short-range wind speed predictions for complex terrain using an interval-artificial neural network. Energy Procedia 2017;125:199–206.
[24] Vapnik V. The Nature of Statistical Learning Theory. Springer Science & Business Media; 2013.
[25] Cheng HY, Yu CC, Lin SJ. Bi-model short-term solar irradiance prediction using support vector regressors. Energy 2014;70:121–7.
[26] Yaslan Y, Bican B. Empirical mode decomposition based denoising method with support vector regression for time series prediction: a case study for electricity load forecasting. Measurement 2017;103:52–61.
[27] Antonanzas J, Urraca R, Martinez-De-Pison FJ, Antonanzas-Torres F. Solar irradiation mapping with exogenous data from support vector regression machines estimations. Energy Convers Manage 2015;100:380–90.
[28] Mohammadi K, Shamshirband S, Anisi MH, Amjad Alam K, Petković D. Support vector regression based prediction of global solar radiation on a horizontal surface. Energy Convers Manage 2015;91:433–41.
[29] Zhao P, Xia J, Dai Y, He J. Wind speed prediction using support vector regression. 2010 5th IEEE Conference on Industrial Electronics and Applications. 2010. p. 882–6.
[30] Ahmadi A, Ehyaei MA. Exergy analysis of a wind turbine. Int J Exergy 2009;6(4):457–76.
[31] Reynaga-lópez RC, Lambert A, Jaramillo O, Zamora M, Leyva E. Exergetic analysis of La Rumorosa-I wind farm rafael. J Fundam Renew Energy Appl 2017;7(1):1–7.
[32] Saravanan AJ. Exergy analysis of single array wind farm using wake effects. Engineering 2011;3(9):949–58.
[33] Öztürk M. Energy and exergy assessments for potential wind power in Turkey. Int J Exergy 2011;8(2):211–26.
[34] Ozgener O, Ozgener L. Exergy and reliability analysis of wind turbine systems: a case study. Renew Sustain Energy Rev 2007;11(8):1811–26.
[35] Baskut O, Ozgener O, Ozgener L. Second law analysis of wind turbine power plants: Cesme, Izmir example. Energy 2011;36(5):2535–42.
[36] Xydis G, Koroneos C, Loizidou M. Exergy analysis in a wind speed prognostic model as a wind farm sitting selection tool: a case study in Southern Greece. Appl Energy 2009;86(11):2411–20.
[37] Baskut O, Ozgener O, Ozgener L. Effects of meteorological variables on exergetic efficiency of wind turbine power plants. Renew Sustain Energy Rev 2010;14(9):3237–41.
[38] Rabbani M, Dincer I, Naterer GF. Thermodynamic assessment of a wind turbine based combined cycle. Energy 2012;44(1):321–8.
[39] Said M, EL-Shimy M, Abdelraheem MA. Improved framework for techno-economical optimization of wind energy production. Sustain Energy Technol Assessments 2017;23:57–72.
[40] Pishgar-Komleh SH, Akram A. Evaluation of wind energy potential for different turbine models based on the wind speed data of Zabol region, Iran. Sustain Energy Technol Assessments 2017;22:34–40.
[41] Quan P, Leephakpreeda T. Assessment of wind energy potential for selecting wind turbines: an application to Thailand. Sustain Energy Technol Assessments 2015;11:17–26.
[42] Hosseinalizadeh R, Sadat Rafiei E, Alavijeh AS, Ghaderi SF. Economic analysis of small wind turbines in residential energy sector in Iran. Sustain Energy Technol Assessments 2017;20:58–71.
[43] Fadai D. The feasibility of manufacturing wind turbines in Iran. Renew Sustain Energy Rev 2007;11(3):536–42.
[44] "IR : Iran Announces New Renewable Energy Facilities - General news news." [Online]. Available: http://www.instalbiz.com/news/1-full-news-ir-iran-announces-new-renewable-energy-facilities_201.html. [Accessed: 04-Jul-2017].
[45] "Renewable Energy and Energy Efficiency Organization." [Online]. Available: http://www.satba.gov.ir/en/home. [Accessed: 05-Jul-2017].
[46] "NASA-SSE - www.soda-pro.com." [Online]. Available: http://www.soda-pro.com/web-services/radiation/nasa-sse. [Accessed: 01-Sep-2017].
[47] Quej VH, Almorox J, Arnaldo JA, Saito L. ANFIS, SVM and ANN soft-computing techniques to estimate daily global solar radiation in a warm sub-humid environment. J Atmos Solar-Terrestrial Phys 2017;155:62–70.
[48] Haznedar B, Kalinli A. Training ANFIS Using Genetic Algorithm for Dynamic Systems Identification. Int J Intell Syst Appl Eng 2016;4(Special issue):44–7.
[49] Oliveira MV, Schirru R. Applying particle swarm optimization algorithm for tuning a neuro-fuzzy inference system for sensor monitoring. Prog Nucl Energy 2009;51(1):177–83.
[50] Betz A. Introduction to the Theory of Flow Machines. Pergamon Press; 1966. p. 167–74.
[51] Şahin AD, Dincer I, Rosen MA. Thermodynamic analysis of wind energy. Int J Energy Res 2006;30(8):553–66.
[52] Bejan A, Tsatsaronis G. Thermal design and optimization. John Wiley & Sons; 1996.
[53] Khosravi A, Koury RNN, Machado L. Thermo-economic analysis and sizing of the components of an ejector expansion refrigeration system. Int J Refrig 2017.